Mathematical Biosciences and Engineering

MBE, 21(1): 765–777.
DOI: 10.3934/mbe.2024032
Received: 06 September 2023
Revised: 26 November 2023
Accepted: 07 December 2023
Published: 19 December 2023

http://www.aimspress.com/journal/MBE

Research article

Generation of stochastic mixed-mode oscillations in a pair of VDP oscillators with direct-indirect coupling

Xiaojun Huang and Zigen Song*

School of Aerospace Engineering and Applied Mechanics, Tongji University, Shanghai 200092, China

* **Correspondence:** Email: zgsong@tongji.edu.cn.

Abstract: Environmental noise can lead to complex stochastic dynamical behavior in nonlinear systems. In this paper, we studied the phenomenon of a pair of Van der Pol (VDP) oscillators with direct-indirect coupling affected by Gaussian white noise. That is to say, a noise-induced equilibrium transition oscillation was observed in three types of different parameter regions, where the deterministic system had two kinds of stable equilibrium points. Meanwhile, with the noise intensity increasing, we found that the stochastic system will constantly switch between two stable equilibrium points. To analyze the stochastic behavior, we used the stochastic sensitivity equation and confidence ellipse method. When the confidence ellipsoid crossed the boundary of the attraction basin of the equilibrium point, the system entered into the state of stochastic mixed-mode oscillations, which was consistent with the simulation results.

Keywords: VDP oscillation; direct-indirect coupling; stochastic dynamic; mixed-mode oscillation; confidence ellipse method; basins of attraction

1. Introduction

As we all know, any real-world dynamic system is influenced by random noise. In fact, noise can give rise to a wide range of complex phenomena, including coherence resonance [1–3], stochastic resonance [4,5], noise-induced bursting [6–8], noise-induced stochastic mixed-mode oscillations [9–11], noise-induce suppression of firing [12], noise-induced chaos and order [13,14], stochastic oscillation bistability in the zone of canard limit cycles [15] and noise-induced transitions between tonic spiking and bursting regimes [16].

For small random perturbations, Fredidlin and Wentzell proposed a large deviation theory to explain the long-term effects of them [17]. Specifically, it is based on the fact that when almost impossible events occur, they occurred along a specific path. This path is called the optimal path which produces the minimum value of some action function. It describes how difficult it is for a random process to pass through the neighborhood of a particular path. The quasi-potential of a particular point is then generated by the action functional along the optimal path of its connection to the attractor. The stochastic sensitivity function and confidence ellipse method was proposed by using the second-order approximation of the potential. It has been successfully used in many systems, such as Hodgkin-Huxley model [12], hair bundle model [9], prey-predator-plankton system [18], Morris-Lecar system [19], Higgins model [20], Hindmarsh-Rose model [21], etc.

The Van der Pol (VDP) oscillator is typical self-excited or self-sustained oscillations, which first originated in vacuum tube circuits. It has been studied in detail in the last century, and the main results can be found in the famous monograph by Nayfeh and Mook [22]. Koshcheev and Vladimir showed the white-noise-induced transition between the limiting cycle and state of rest of a VDP oscillator that has a threshold, and the threshold value is directly proportional to the product of the characteristic energy of self-oscillations and the friction coefficient [23]. For the coupled VDP oscillator, some coupling schemes are used, including weak coupling with delay [24], indirect coupling [25] and dynamic coupling [26]. In the direct-indirect coupling VDP oscillator coupling system, we have found a wealth of kinetic phenomena [26]. If we introduce noise into it, we find more dynamics in it. In this paper, we show the noise-induced escape on a direct-indirect coupled pair of VDP systems and generate mixed-mode stochastic oscillations.

This paper is organized as follows. We first propose a mathematical model of the pair of VDP oscillator systems with direct-indirect coupling and give its equilibrium distribution with changing parameters in Section 2. In Section 3, we show the oscillations of the corresponding random system under different noise intensities. In Section 4, we give the reason of this phenomenon by using random sensitivity matrix and confidence ellipse method. Conclusions and discussions are given in Section 5.

2. Deterministic model

In this paper, we investigate the VDP coupled system with two types of connections, i.e., a direct and an indirect coupling. The direct coupling is diffusive mutually coupling, and the indirect coupling is carried by using external environment. The system dynamics is presented [27] as

$$\begin{cases} dx_{11}/dt = x_{12} + d(x_{21} - x_{11}) + ey, \\ dx_{12}/dt = a(1 - x_{11}^2)x_{12} - x_{11}, \\ dx_{21}/dt = x_{22} + d(x_{11} - x_{21}) + ey, \\ dx_{22}/dt = a(1 - x_{21}^2)x_{22} - x_{21}, \\ dy/dt = -ky - e(x_{11} + x_{21})/2, \end{cases} \tag{1}$$

where x_{i1}, x_{i2} are firing activities of the i-th oscillator, a is a nonlinear damping ratio of the individual oscillator, d is a coupling strength of direct coupling, the state variable y denotes indirect coupling of the external environment, which is modeled by a one-dimensional over-damped oscillator with

damping parameter k and the parameter e is a coupling strength between systems and environment.

We carry out the equilibrium analysis of system (1) and obtain the following equations:

$$\begin{cases} x_{12}+d(x_{21}-x_{11})+ey=0, \\ a(1-x_{11}^2)x_{12}-x_{11}=0, \\ x_{22}+d(x_{11}-x_{21})+ey=0, \\ a(1-x_{21}^2)x_{22}-x_{21}=0, \\ -ky-e(x_{11}+x_{21})/2=0. \end{cases}$$

By solving the above equation, we get four types of equlibrium points, including the origin O (0, 0, 0, 0, 0), inhomogeneous steady state (IHSS) $A^{\pm}\left(\pm x_{11}^A, \pm x_{12}^A, \mp x_{11}^A, \mp x_{12}^A, 0\right)$, homogeneous steady state (HSS) $B^{\pm}\left(\pm x_{11}^B, \pm x_{12}^B, \pm x_{11}^B, \pm x_{12}^B, \mp y^B\right)$ and no-pattern steady state (NPSS) $C^{\pm}\left(\pm x_{11}^C, \pm x_{12}^C, \mp x_{21}^C, \mp x_{22}^C, \pm y^C\right)$, $D^{\pm}\left(\pm x_{11}^D, \pm x_{12}^D, \mp x_{21}^D, \mp x_{22}^D, \pm y^D\right)$, where $x_{11}^A=\sqrt{2ad-1}/\sqrt{2ad}$, $x_{12}^A=\pm\sqrt{2d}\sqrt{2ad-1}/\sqrt{a}$, $x_{11}^B=\sqrt{ae^2-k}/e\sqrt{a}$, $x_{12}^B=e\sqrt{ae^2-k}/k\sqrt{a}$ and $y^B=\sqrt{ae^2-k}/k\sqrt{a}$. Because $C^{\pm}$ and $D^{\pm}$ are more complex, they are not listed here.

In order to show the distribution position and the properties of the equilibrium points, we fix $a=1, d=1, k=1.3$ in this paper, and consider the dynamics of system (1) under different values of parameter e. When $e>1.2465$, the system enters the equilibrium state. There are three types of equilibria: A pair of IHSS equilibria $A^{\pm}$, a pair of HSS equilibria $B^{\pm}$ and trivial equilibrium O. $A^{\pm}$ are stable equilibrium points. $B^{\pm}$ and O are unstable equilibrium points. A pitchfork bifurcation occurs, adding four unstable equilibrium points: NPSS equilibria $C^{\pm}$ and $D^{\pm}$. Next, when $e=1.6125$, the equilibria $B^{\pm}$ gains stability. Finally, an anti-pitchfork bifurcation appears, the points $C^{\pm}$ and $D^{\pm}$ disappear, and the points $A^{\pm}$ lose their stability, leaving only a pair of stable equilibria $B^{\pm}$.

Figure 1 shows three examples of different types of stable equilibria in the deterministic system characterized by the nullclines. As can be seen from Figure 1(a), when $e=1.28$, there are five equilibrium points in the system: Unstable points O and $B^{\pm}$ and stable fixed points $A^{\pm}$. When $e=1.9$, as shown in Figure 1(b), there are two pairs of stable fixed points of the system: $A^{\pm}$ and $B^{\pm}$, respectively. The unstable point is the point O, and there are two pairs of saddle points: $C^{\pm}$ and $D^{\pm}$. When $e=3$, as shown in Figure 1(c), the system re-obtains the stable equilibrium points $B^{\pm}$, where $A^{\pm}$ are saddle points, and O is an unstable point. At the same time, the corresponding phase diagrams for different values of parameter e with different initial values are given, as shown in Figure 2. It can be observed that for the fixed parameters of the system, different initial values can make the system fall into different equilibrium points.

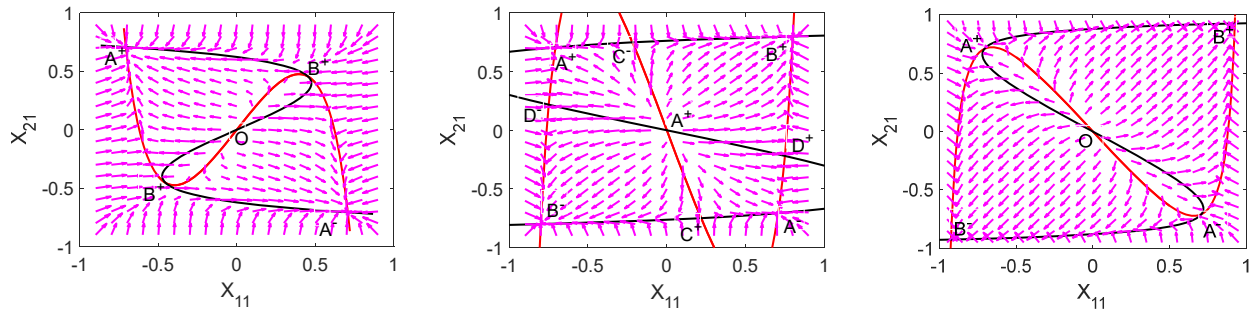

(a) (b) (c)

Figure 1. The intersection points of the system's nullclines and vector field show number of equilibria with the fixed parameter (a) e = 1.28, (b) e = 1.9, (c) e = 3, where O is the trivial equilibrium, $A^{\pm}$ means the IHSS equilibrium, $B^{\pm}$ means the HSS equilibrium, and $C^{\pm}$ and $D^{\pm}$ are the NPSS equilibria.

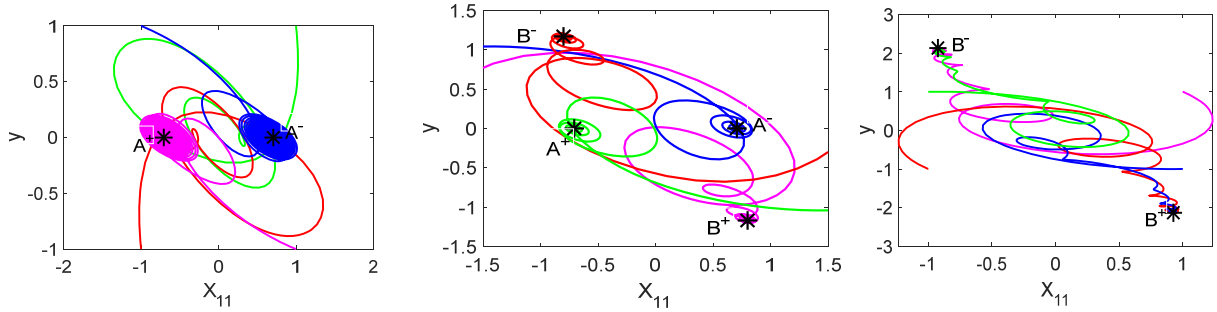

(a) (b) (c)

Figure 2. Phase diagrams (a) e = 1.28 with initial values (–1,0,0,0,–1), (–1,0,0,0,1), (1,0,0,0,–1) and (1,0,0,0,1); (b) e = 1.9 with (–2,0,0,0,–2), (–2,0,0,0,1), (2,0,0,0,1) and (2,0,0,0,2); (c) e = 3 with (–1, 0,0,0,–1), (–1,0,0,0,1), (1,0,0,0,–1) and (1,0,0,0,1) for the fixed parameters a = 1, d = 1, k = 1.3.

3. Stochastic model

Let us examine how random noise changes the system dynamics of model (1). Here we will study the following stochastic model:

$$\begin{cases} dx_{11}/dt = x_{12} + d(x_{21} - x_{11}) + ey, \\ dx_{12}/dt = a(1 - x_{11}^2)x_{12} - x_{11}, \\ dx_{21}/dt = x_{22} + d(x_{11} - x_{21}) + ey, \\ dx_{22}/dt = a(1 - x_{21}^2)x_{22} - x_{21}, \\ dy/dt = -ky - e(x_{11} + x_{21})/2 + \varepsilon\xi(t), \end{cases} \tag{2}$$

where $\xi(t)$ is a standard Gaussian white noise with $E\xi(t) = 0, E\xi(t)\xi(\tau) = \delta(t - \tau)$ and ε is a noise intensity parameter.

In order to illustrate the effect of Gaussian white noise, we focus on the stochastic phenomena

for the different values of parameter e with small and large noise intensity. For the numerical simulations of random trajectories, we use the Euler-Maruyama scheme with the time step 0.01 in accordance with practice.

Figure 3 illustrates the random phase trajectories and the corresponding history series with $e = 1.28, 1.9, 3$ for the low noise intensity $\varepsilon = 0.02$. We can obviously find that the random trajectories vibrate in the neighborhood of the stable fixed points and form dispersion. Further, the small noise intensity does not change the overall property of the model. However, the system enters a switch of equilibrium points under large noise intensity, as shown in Figure 4, where the history series are to the parameters $e = 1.28, \varepsilon = 0.2$, $e = 1.9, \varepsilon = 0.5$ and $e = 3, \varepsilon = 1$, respectively. As can be seen from the figures, we can observe large amplitude stochastic oscillations around the equilibrium point and random switching between the two equilibrium points. The noise-induced transition phenomenon is observed.

Figure 5 shows the relationship between noise intensity and the coordinate of the stochastic system. The figure depicted here has its horizontal axis representing the intensity of noise, while the vertical axis corresponds to x_{11}. The system begins integrating at a noise intensity of zero, and subsequently carries out the same operation at intervals of $\log_{10}(0.01)$. This process illustrates the range of coordinate x_{11} of the system. As can be seen, when the noise intensity is very small, the oscillation amplitude caused by the random noise is also very small. The greater the noise intensity, the greater the amplitude of the oscillation. After the noise intensity of different threshold values, the random system will enter the noise-induced large amplitude oscillation.

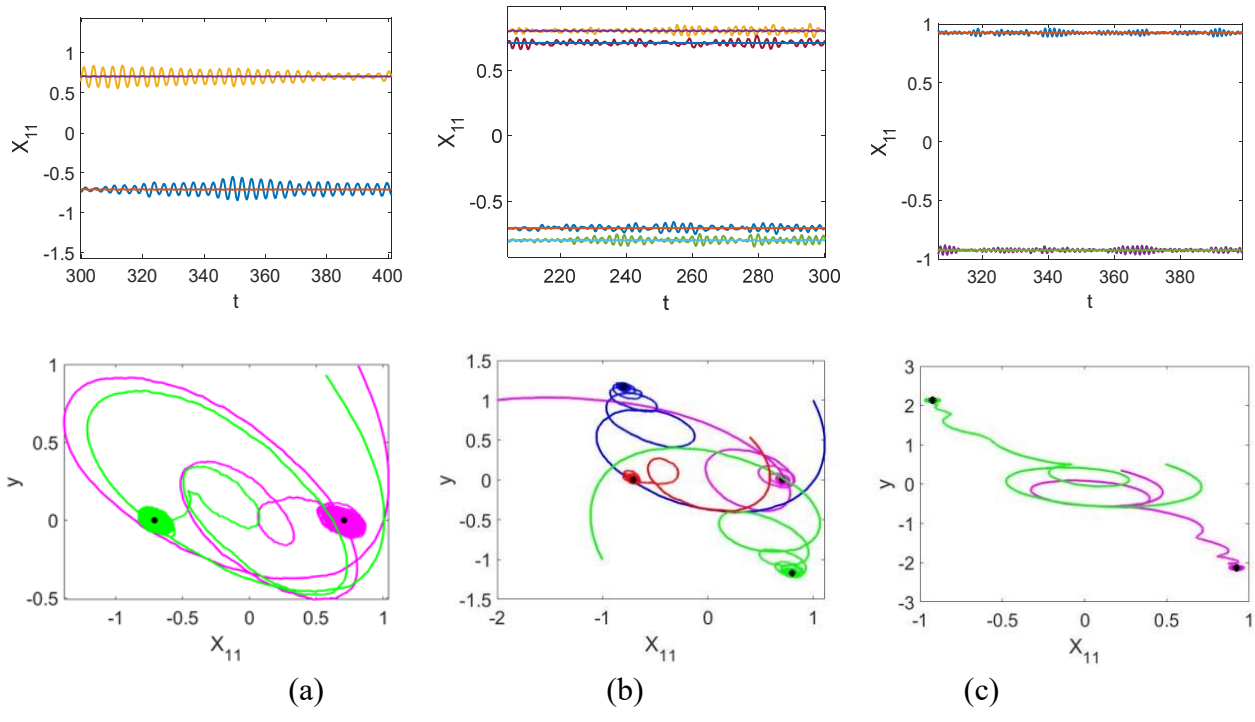

Figure 3. (Up) The history series of the stochastic system and corresponding deterministic system and (Down) phase diagram with (a) $e = 1.28$, (b) $e = 1.9$, (c) $e = 3$, where the system parameter values are $a = 1$, $d = 1$, $k = 1.3$ for the noise intensity 0.02.

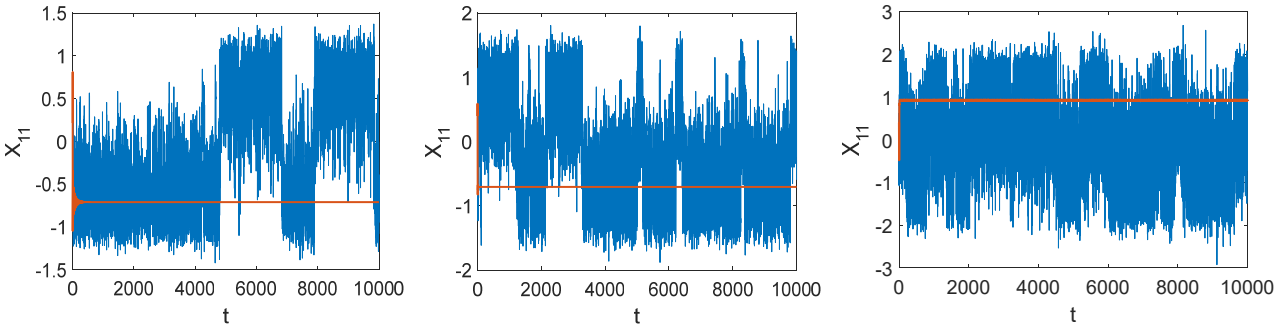

(a) (b) (c)

Figure 4. Time history diagrams of the stochastic system (2) with (a) $e = 1.28,\ \varepsilon = 0.2$, (b) $e = 1.9,\ \varepsilon = 0.5$, and (c) $e = 3,\ \varepsilon = 1$.

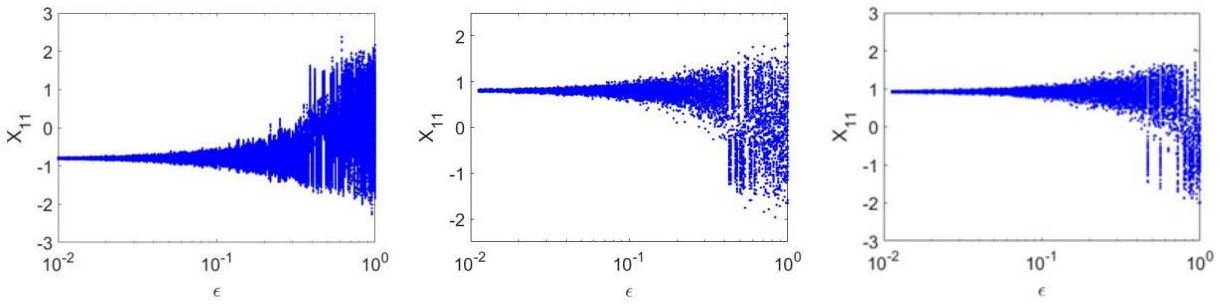

(a) (b) (c)

Figure 5. Bifurcation diagram of the noise intensity for (a) e = 1.28, (b) e = 1.9, and (c) e = 3.

4. Stochastic sensitivity analysis

In this section, we first give the attraction basins of all equilibria for $e = 1.28, 1.9, 3$ in the deterministic system (1), as shown in Figure 6. As shown in the figure, areas of different colors represent the attraction basins of different equilibrium points. We take an interval of 0.01, with the value range of x_{11} and x_{21} being –2 to 2, and set the initial values to satisfy equation (2). Numerical integration is performed using the Runge-Kutta algorithm. If the system falls into the same equilibrium point, the corresponding point will be painted with the same color. As can be seen, the position of the stable fixed point, which the system finally stays in, depends on the position of the initial point of the deterministic system. Meanwhile, there are some boundary surfaces between different basins. If the trajectory of random system (2) crosses the basin of attraction, the system will inevitably fall into another equilibrium point. In stochastic systems, random terms will cause perturbations to phase trajectories. The larger the random coefficient, the larger the range of random system disturbance. If the perturbation of a random system breaks through the boundary of the attractive disk, the system will inevitably fall into another equilibrium point of the attractive disk range. The system vibrates up and down around another equilibrium point.

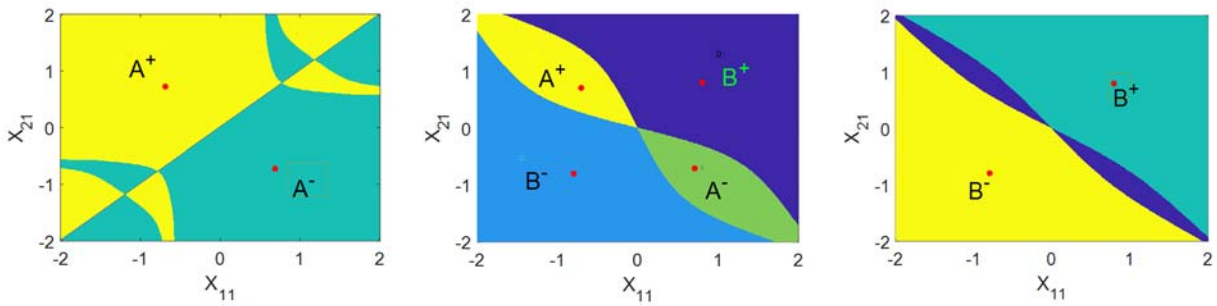

(a) (b) (c)

Figure 6. The attraction basins of all equilibria for (a) $e=1.28$, (b) $e=1.9$, (c) $e=3$.

In order to analyze the noise-induced random oscillation, we use the confidence ellipse method based on the stochastic sensitivity matrix technique [27]. The technique of the stochastic sensitivity matrix that we employ is fundamentally developed on the basis of the Hamilton-Jacobi equation. Before analyzing, we give the Jacobian matrix of the deterministic system (1).

$$J=\begin{pmatrix} -d & 1 & d & 0 & e \\ -2ax_{11}x_{12}-1 & a(1-x_{11}^2) & 0 & 0 & 0 \\ d & 0 & -d & 1 & e \\ 0 & 0 & -1-2ax_{21}x_{22} & a(1-x_{21}^2) & e \\ -e/2 & 0 & -e/2 & 0 & -k \end{pmatrix}. \tag{3}$$

The random sensitivity matrix W of the stable equilibrium point $(x_{11},x_{12},x_{21},x_{22},y)$ for the deterministic system (1) can be obtained by the following matrix equation:

$$JW+WJ^T+S=0,\quad S=\begin{pmatrix} 0 & 0 & 0 & 0 & 0 \\ 0 & 0 & 0 & 0 & 0 \\ 0 & 0 & 0 & 0 & 0 \\ 0 & 0 & 0 & 0 & 0 \\ 0 & 0 & 0 & 0 & 1 \end{pmatrix}. \tag{4}$$

The random sensitivity matrix of the different stable fixed points can be obtained by solving the corresponding matrix equation. Using the matrix W, one can write an asymptotic of the time-varying probability density function

$$\rho(\mathbf{x},\varepsilon)\approx k\exp(-\frac{[\mathbf{x}-\bar{\mathbf{x}},W^{-1}(\mathbf{x}-\bar{\mathbf{x}})]}{2\varepsilon}). \tag{5}$$

The eigenvalues and eigenvectors can form the confidence ellipse of the corresponding points. The eigenvalue determines the semi-axis of the confidence ellipse, and the eigenvector determines the direction axis of the corresponding confidence ellipse. Let $\mu_1,\mu_2,\mu_3,\mu_4,\mu_5$ be eigenvalues and u_1,u_2,u_3,u_4,u_5 be the normalized eigenvectors of the stochastic sensitivity matrix. For coordinates z_1,z_2,z_3,z_4,z_5 of the confidence ellipse in the basis u_1,u_2,u_3,u_4,u_5 with the equilibrium as the origin,

we have the following equation:

$$\frac{z_1^2}{\mu_1}+\frac{z_2^2}{\mu_2}+\frac{z_3^2}{\mu_3}+\frac{z_4^2}{\mu_4}+\frac{z_5^2}{\mu_5}=\varepsilon K(P), \tag{6}$$

where ε is the noise intensity and $K(P)$ is the confidence probability function.

4.1. Random sensitivity analysis of the equailibrium points $A^{\pm}$

Substituting the equilibrium point $A^{\pm}$ into the matrix equation, we can solve the corresponding random sensitivity matrix:

$$W_A=\begin{pmatrix}
\frac{e^2(1+4e^2-26k)}{2\Delta_3} & \frac{3e^2(1-2k)}{\Delta_3} & \frac{e^2(1+4e^2-26k)}{2\Delta_3} & \frac{3e^2(1-2k)}{\Delta_3} & \frac{3e(-1+2k)}{\Delta_3}\\
\frac{3e^2(1-2k)}{\Delta_3} & \frac{18e^2(1-2k)}{\Delta_3} & \frac{3e(-1+2k)}{\Delta_3} & \frac{18e^2(1-2k)}{\Delta_3} & \frac{6e(-3+e^2)}{\Delta_3}\\
\frac{e^2(1+4e^2-26k)}{2\Delta_3} & \frac{3e^2(1-2k)}{\Delta_3} & \frac{e^2(1+4e^2-26k)}{2\Delta_3} & \frac{3e^2(1-2k)}{\Delta_3} & \frac{3e(-1+2k)}{\Delta_3}\\
\frac{3e^2(1-2k)}{\Delta_3} & \frac{18e^2(1-2k)}{\Delta_3} & \frac{3e(-1+2k)}{\Delta_3} & \frac{18e^2(1-2k)}{\Delta_3} & \frac{6e(-3+e^2)}{\Delta_3}\\
\frac{3e(-1+2k)}{\Delta_3} & \frac{6e(-3+e^2)}{\Delta_3} & \frac{3e(-1+2k)}{\Delta_3} & \frac{6e(-3+e^2)}{\Delta_3} & \frac{36+4e^4+6k(-1+2k)-e^2(11+26k)}{2\Delta_3}
\end{pmatrix}, \tag{7}$$

where $\Delta_3=2(e^2-6k)(-6+k+4e^2k-2k^2)$. It is easy to know that when $e=\sqrt{6k}$ or $e=\sqrt{(6-k+2k^2)/4k}$, i.e., $e=1.2465$ or $e=2.7928$, the random system will immediately enter the random oscillation state. Here, when we set $e=1.2465$, points $A^{\pm}$ turn into the stable equilibrium points and when we set $e=2.7928$, points $A^{\pm}$ lose their stability. Figure 7 shows the eigenvalue of the stochastic sensitivity matrix of the equilibrium point $A^{\pm}$ described by the function with parameter e as the independent variable. It is obvious that the random sensitivity of the system will change with the system parameter e. However, when e approaches 1.2465 or 2.7928, the random sensitivity of the system increases indefinitely.

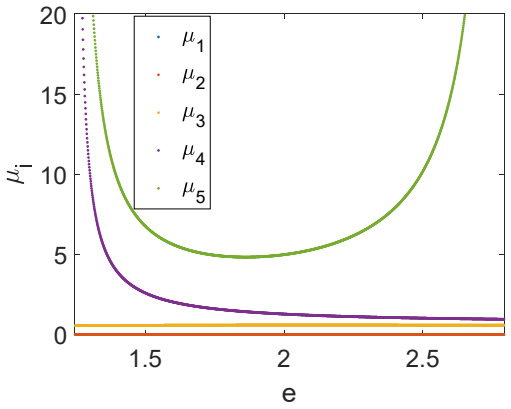

Figure 7. Eigenvalue function of the stochastic sensitivity matrix for the equilibrium point $A^{\pm}$.

Figure 8 also shows the confidence ellipses when we set $e=1.28, 1.9$ and $\varepsilon=0.1, 0.2$. As can be seen from the figure, when we set $\varepsilon=0.1$, the confidence ellipses are still in the basin of attraction for the corresponding equilibrium, but when we set $\varepsilon=0.2$, the confidence ellipses become larger and cross the dividing line into the attraction basin of another equilibrium state. As can be seen from Figure 8(a), the random trajectory will enter into another IHSS equilibrium. The random trajectory oscillates back and forth between the equilibrium $A^{\pm}$. In Figure 8(b), when we set $\varepsilon=0.2$, the random trajectory will be equally possible to enter into the HSS equilibria $B^{\pm}$. The motion of the stochastic system at the equilibria $B^{\pm}$ will be given in the calculation results in the following subsection. Figure 9 shows the time history diagram and stochastic bifurcation diagram of the corresponding stochastic system.

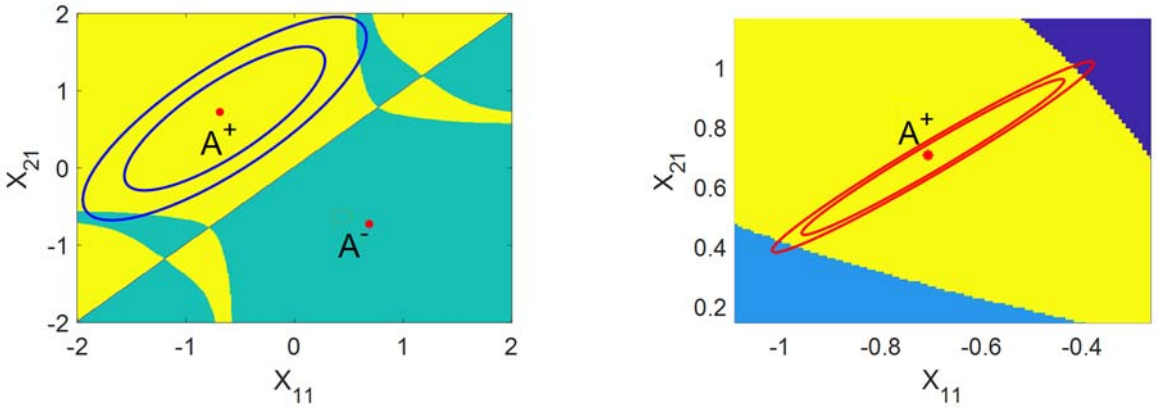

(a) (b)

Figure 8. The attraction basin of equilibrium A^{+} (by color) and the corresponding confidence ellipse for $\varepsilon=0.1$ (small ellipse) and $\varepsilon=0.2$ (large ellipse) in the deterministic system with the fixed parameter (a) $e=1.28$ and (b) $e=1.9$.

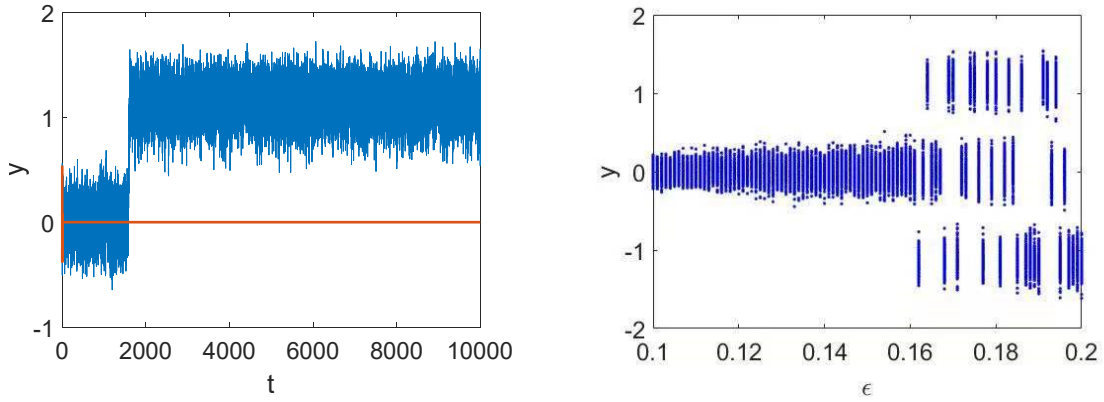

(a) (b)

Figure 9. (a) Time history diagrams for $e=1.9$ and $\varepsilon=0.2$. (b) Bifurcation diagram between the noise intensity and the coordinate y.

4.2. Random sensitivity analysis of the equailibrium points $B^{\pm}$

Considering the random sensitivity matrix equation corresponding to the equilibrium point $B^{\pm}$, we get the following random senstivity matrix:

$$W_B = \begin{pmatrix} \frac{2e^8-2e^6k+(-1+e^2)k^3}{\Delta_4} & \frac{e^2(-1+e^2)(2e^2-k)k}{\Delta_4} & \frac{2e^8-2e^6k+(-1+e^2)k^3}{\Delta_4} & \frac{e^2(-1+e^2)(2e^2-k)k}{\Delta_4} & -\frac{e(-1+e)(2e^2-k)k}{\Delta_4} \\ \frac{e^2(-1+e^2)(2e^2-k)k}{\Delta_4} & \frac{e^4(-1+e^2)(2e^2+k)^2}{\Delta_4} & \frac{e^2(-1+e^2)(2e^2-k)k}{\Delta_4} & \frac{e^4(-1+e^2)(2e^2+k)^2}{\Delta_4} & \frac{e^3(2e^2-k)(e^2(-2+k)+k)}{\Delta_4} \\ \frac{2e^8-2e^6k+(-1+e^2)k^3}{\Delta_4} & \frac{e^2(-1+e^2)(2e^2-k)k}{\Delta_4} & \frac{2e^8-2e^6k+(-1+e^2)k^3}{\Delta_4} & \frac{e^2(-1+e^2)(2e^2-k)k}{\Delta_4} & -\frac{e(-1+e)(2e^2-k)k}{\Delta_4} \\ \frac{e^2(-1+e^2)(2e^2-k)k}{\Delta_4} & \frac{e^4(-1+e^2)(2e^2+k)^2}{\Delta_4} & \frac{e^2(-1+e^2)(2e^2-k)k}{\Delta_4} & \frac{e^4(-1+e^2)(2e^2+k)^2}{\Delta_4} & \frac{e^3(2e^2-k)(e^2(-2+k)+k)}{\Delta_4} \\ -\frac{e(-1+e^2)(2e^2-k)k}{\Delta_4} & -\frac{e^3(2e^2-k)(e^2(-2+k)+k)}{\Delta_4} & -\frac{e(-1+e^2)(2e^2-k)k}{\Delta_4} & -\frac{e^3(2e^2-k)(e^2(-2+k)+k)}{\Delta_4} & \frac{1}{4}\left(\frac{1}{e^2-k}+\frac{2}{k}+\frac{-e^4(-2+k)-e^2(-1+k)k+k^2}{-2e^4+e^6k+k^3+e^2(k-k^3)}\right) \end{pmatrix}, \quad (8)$$

where $\Delta_4 = 4(e^2-k)(-2e^4+e^6k+k^3+e^2(k-k^3))$. However, when HSS equilibria $B^{\pm}$ enters the stable state, $\Delta_4 > 0$. Figure 10 shows the eigenvalue of the stochastic sensitivity matrix of the equilibrium points $B^{\pm}$ described by the function with parameter e as the independent variable. Similar to Figure 7, the random sensitivity of the system will change as e changes.

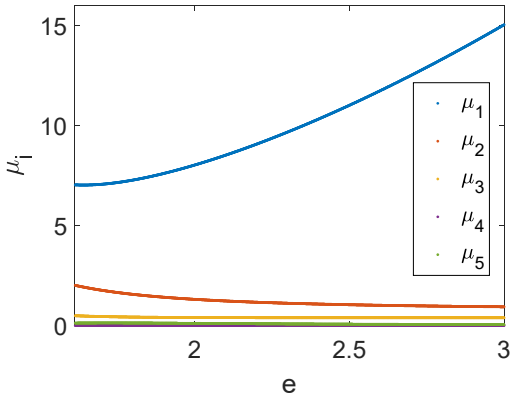

Figure 10. Eigenvalue function of the random sensitivity matrix for the equilibrium point $B^{\pm}$.

Figure 11 shows the confidence ellipses of the large and small noise intensity when the point $B^{\pm}$ are stable fixed points. The confidence ellipse then degenerates into a line segment. As can be seen from the figure, when we set $e = 1.9$ and $\varepsilon = 0.3$, the confidence ellipse is still in the basin of attraction of the corresponding equilibrium, but when $\varepsilon = 0.5$, the confidence ellipse becomes larger and crosses the boundary entering into the attraction basin of the another equilibrium. The random trajectory of system (2) jumps back and forth between B^{+} and B^{-}. However, due to the property of the confidence ellipse, the system cannot jump into the equilibrium point $A^{\pm}$. When we set $e = 3$ and $\varepsilon = 0.5$, the random will not cause the transition between two equilibria. Further, when $\varepsilon = 1$, the phenomenon of transition of the equilibrium point can be observed. The corresponding time history is shown in Figure 4 (c).

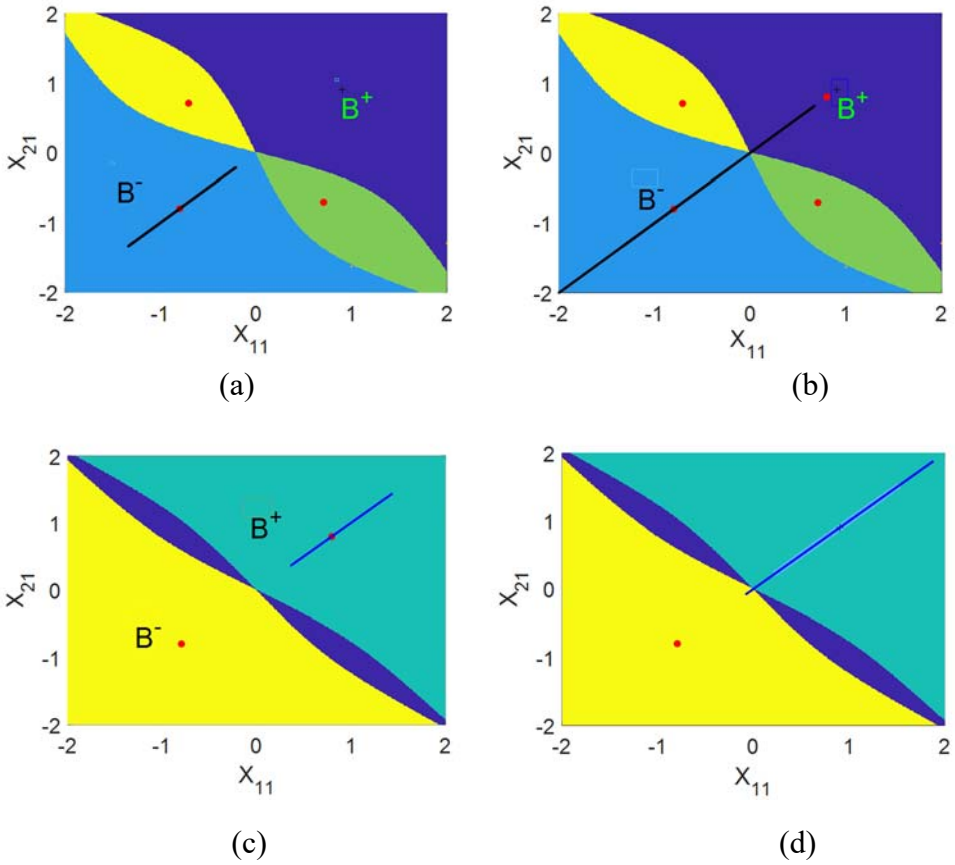

Figure 11. The confidence ellipse described by the attraction basin of the equilibrium point $B^{\pm}$ for the deterministic system with (a) $e=1.9$, $\varepsilon=0.3$ (b) $e=1.9$, $\varepsilon=0.5$, (c) $e=3$, $\varepsilon=0.5$, and (d) $e=3$, $\varepsilon=1$.

5. Conclusions and discussions

The phenomenon of a pair of VDP oscillator affected by Gaussian white noise was studied. In this paper, we showed that the random noise can produce mixed-mode oscillations in the parameter region for the deterministic model having only the stable equilibrium point as the attractor. The phenomenon of spontaneous mixed-mode oscillation induced by noise was studied using the semi-analytic method based on the random sensitivity function and confidence ellipse.

The results showed that the mechanism of this phenomenon can be explained by the specificity of the attraction basin and the random sensitivity of the equilibrium point. When a random noise term was introduced into the system, the system vibrated around the equilibrium point. The greater the random noise intensity, the larger the confidence ellipse of system vibration. When the confidence ellipse crossed the boundary of the attraction basin at that point, the system would no longer vibrate around this equilibrium point. It jumped into a different equilibrium point. It is worth noting that when the system parameters allowed the system to have two equilibrium points of $A^{\pm}$ and $B^{\pm}$, the deterministic system at $A^{\pm}$ would vibrate around the equilibrium point of $B^{\pm}$ and would not return to $A^{\pm}$ after the random strength became more larger. This article can give us a better understanding of the behavior of nonlinear dynamical systems. This study opened up new avenues for further research. For example, it would be very interesting to study how different types of noise (e.g., Gaussian noise, Poisson noise, etc.) affect the behavior of VDP oscillators and other similar systems.

Use of AI tools declaration

The authors declare they have not used Artificial Intelligence (AI) tools in the creation of this article.

Acknowledgments

This research is supported by the National Natural Science Foundation of China (No. 12172212) and the Fundamental Research Funds for the Central Universities (No. 22120220588).

Conflict of interest

The authors declare there is no conflict of interest.

References

1. A. S. Pikovsky, J. Kurths, Coherence resonance in a noise-driven excitable system, *Phys. Rev. Lett.*, **78** (1997), 775. https://doi.org/10.1103/PhysRevLett.78.775
2. A. N. Pisarchik, A. E. Hramov, Coherence resonance in neural networks: Theory and experiments. *Phys. Rep.*, **1000** (2023), 1–57. https://doi.org/10.1016/j.physrep.2022.11.004
3. Z. Q. Wang, Y. Xu, H. Yang, Lévy noise induced stochastic resonance in an FHN model, *Sci. China Technol. Sci.*, **59** (2016), 371–375. https://doi.org/10.1007/s11431-015-6001-2
4. M. D. McDonnell, D. Abbott, What is stochastic resonance? Definitions, misconceptions, debates, and its relevance to biology, *PLoS Comput. Biol.*, **5** (2009), e1000348. https://doi.org/10.1371/journal.pcbi.1000348
5. A. Calim, T. Palabas, M. Uzuntarla, Stochastic and vibrational resonance in complex networks of neurons, *Philos. T. R. Soc. A*, **379** (2021), 20200236. https://doi.org/10.1098/rsta.2020.0236
6. I. Bashkirtseva, L. Ryashko, E. Slepukhina, Noise-induced spiking-bursting transition in the neuron model with the blue sky catastrophe, *Phys. Rev. E*, **99** (2019), 062408. https://doi.org/10.1103/PhysRevE.99.062408
7. E. Slepukhina, I. Bashkirtseva, L. Ryashko, Stochastic spiking-bursting transitions in a neural birhythmic 3D model with the Lukyanov-Shilnikov bifurcation, *Chaos Soliton Fract.*, **138** (2020), 109958. https://doi.org/10.1016/j.chaos.2020.109958
8. E. Slepukhina, I. Bashkirtseva, L. Ryashko, P. Kügler, How noise transforms spiking into bursting in a neuron model having the Lukyanov-Shilnikov bifurcation, *Commun. Nonlinear Sci.*, **118** (2023), 106992. https://doi.org/10.1016/j.cnsns.2022.106992
9. I. Bashkirtseva, L. Ryashko, Generation of mixed-mode stochastic oscillations in a hair bundle model, *Phys. Rev. E*, **98** (2018), 042414. https://org/doi/10.1103/PhysRevE.98.042414
10. I. Bashkirtseva, L. Ryashko, Mixed-mode self-oscillations, stochastic excitability, and coherence resonance in flows of highly concentrated suspensions, *Nonlinear Dyn.*, **102** (2020), 1837–1848. https://doi.org/10.1007/s11071-020-06025-3
11. I. Bashkirtseva, Stochastic sensitivity analysis of mixed-mode oscillations in kinetics of the flow reactor, *Math. Method Appl. Sci.*, **44** (2021), 12047–12057. https://doi.org/10.1002/mma.6546

12. I. Bashkirtseva, A. B. Neiman, L. Ryashko, Stochastic sensitivity analysis of noise-induced suppression of firing and giant variability of spiking in a Hodgkin-Huxley neuron model, *Phys. Rev. E*, **91** (2015), 052920. https://org/doi/10.1103/PhysRevE.91.052920
13. I. Bashkirtseva, L. Ryashko, E. Slepukhina, Order and chaos in the stochastic Hindmarsh-Rose model of the neuron bursting, *Nonlinear Dyn.*, **82** (2015), 919–932. https://doi.org/10.1007/s11071-015-2206-y
14. I. Bashkirtseva, V. Nasyrova, L. Ryashko, Noise-induced bursting and chaos in the two-dimensional Rulkov model, *Chaos Soliton Fract.*, **110** (2018), 76–81. https://doi.org/10.1016/j.chaos.2018.03.011
15. I. Bashkirtseva, L. Ryashko, How noise can generate calcium spike-type oscillations in deterministic equilibrium modes, *Phys. Rev. E.*, **105** (2022), 054404. https://org/doi/10.1103/PhysRevE.105.054404
16. L. B. Ryashko, E. S. Slepukhina, Analysis of noise-induced transitions between spiking and bursting regimes in Hindmarsh-Rose neuron model, in *CEUR Workshop Proceedings*, **1662** (2016), 306–314.
17. M. I. Freidlin, A. D. Wentzell, M. I. Freidlin, A. D. Wentzell, Random perturbations, in *Random Perturbations of Dynamical Systems*, New York, (2012), 15–43. https://doi.org/10.1007/978-1-4612-0611-8_2
18. I. Bashkirtseva, L. Ryashko, Stochastic sensitivity analysis of noise-induced excitement in a prey-predator plankton system, *Front. Life Sci.*, **5** (2011), 141–148. https://doi.org/10.1080/21553769.2012.702666
19. L. Ryashko, Sensitivity analysis of the noise-induced oscillatory multistability in Higgins model of glycolysis, *Chaos*, **28** (2018), 033602. https://doi.org/10.1063/1.4989982
20. E. Slepukhina, I. Bashkirtseva, P Kugler, L. Ryashko, Noise-driven bursting birhythmicity in the Hindmarsh-Rose neuron model, *Chaos*, **33** (2023), 033106. https://doi.org/10.1063/5.0134561
21. A. H. Nayfeh, D. T. Mook, *Nonlinear oscillations*, John Wiley & Sons, New York, 1979.
22. S. Wirkus, R. Rand, The dynamics of two coupled van der Pol oscillators with delay coupling, *Nonlinear Dyn.*, **30** (2002), 205–221. https://doi.org/10.1023/A:1020536525009
23. V. P. Koshcheev, Noise-induced transition between stationary states of a van der Pol oscillator, *Tech. Phys. Lett.*, **40** (2014), 126–128. https://doi.org/10.1134/S1063785014020114
24. E. Camacho, R. Rand, H. Howland, Dynamics of two van der Pol oscillators coupled via a bath, *Int. J. Solids Struct.*, **41** (2004), 2133–2143. https://doi.org/10.1016/j.ijsolstr.2003.11.035
25. K. Konishi, Experimental evidence for amplitude death induced by dynamic coupling: van der Pol oscillators, in *2004 IEEE International Symposium on Circuits and Systems (ISCAS)*, (2004), IV–792. https://doi.org/10.1109/ISCAS.2004.1329123
26. V. Resmi, G. Ambika, R. E. Amritkar, General mechanism for amplitude death in coupled systems, *Phys. Rev. E*, **84** (2011), 046212. https://org/doi/10.1103/PhysRevE.84.046212
27. I. Bashkirtseva, L. Ryashko, Analysis of excitability for the FitzHugh-Nagumo model via a stochastic sensitivity function technique, *Phys. Rev. E*, **83** (2011), 061109. https://org/doi/10.1103/PhysRevE.83.061109

AIMS Press